

Electrochemical Generation of Ozone: Comparison of IrO₂ series with Pt/SnO₂ anode support in solid membrane cell

Chi-Wen Chen, Ay Su, Chia-Chen Yeh, Jyun-Wei Yu, Yu-Ting Lu, Guo-Bin Jung*

Yuan Ze University, 135 Yuan-Tung Road, Chung-Li, Taiwan 32003, R.O.C.

*E-mail: guobin@saturn.yzu.edu.tw

Received: 28 July 2015 / Accepted: 29 February 2015 / Published: 1 April 2016

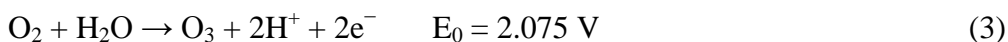
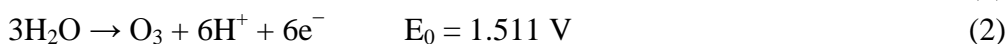
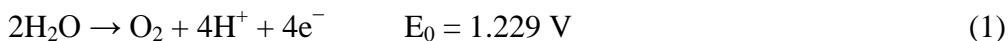
The technology of Proton exchange membrane water electrolysis offers an alternative to the corona discharge technology by preventing nitrogen oxide formation during ozone generation. In this study, various anode supports were installed in the membrane cell and their ozone production performances were assessed. The Pt/IrO₂, Ta/IrO₂ and Ru/IrO₂ were compared with Pt/SnO₂ based used for ozone generation specially in solid membrane cell, to be a anode support. An important component of the membrane cell for ozone generation, the anode support should exhibit corrosion resistance, oxygen evolution activity, good electrical conductivity, electrochemical stability, and low oxygen evolution over potential. The result shows Pt/SnO₂ ozone anode support has better performance than Pt/IrO₂, Ta/IrO₂ and Ru/IrO₂ anode supports,.

Keywords: electrochemical, ozone, electrolysis

1. INTRODUCTION

Ozone was an inorganic pale blue gas with a distinctively pungent smell. This allotrope of oxygen, which makes up only 0.6 ppm of the Earth's atmosphere, was useful for many applications, such as water treatment, sterilization, odor control, medical therapy, color removal, disinfection, agriculture, and food processing and storage, because of its strong oxidizing ability and low persistence [1]. In addition to generating ozone, the typical corona discharge technology produces nitrogen oxides (NO_x), prompting an active search for alternate synthetic approaches toward ozone. Electrochemical ozone production has been extensively investigated as a substitute for corona discharge [2-11] but requires more energy than the conventional process [4]. Conversely, a proton exchange membrane water electrolyzer (PEMWE) directly generates ozone from pure water without NO_x formation. The ozone formation reactions during the electrolysis of water are as follows [12]:

Anode:



Cathode:



As shown in Eqs. (1)–(4), the electrolysis of water generates oxygen, ozone, and protons at the anode. These protons move through the membrane toward the cathode, where hydrogen evolution finally occurs. This method exclusively requires pure water as feedstock and only emits ozone, oxygen, and hydrogen, making it environmental friendly [13].

Numerous types of solid electrodes [2], such as Pt, PbO₂, TiO₂ [14], and SnO₂-based electrodes [15], have been implemented in PEMWEs for ozone production. Their performance hinges on mechanical stability and uniform current distribution. Most importantly, their composition requires a significant amount of expensive platinum-group metal oxide electro catalysts, such as IrO₂ and RuO₂ [16]. Because of the high over potential, the presence of oxygen, and the acidic environment, PEMWEs demand a corrosion resistant anode that exhibits good electrical conductivity and porosity to promote water transport and gas removal [17].

Grigoriev et al. [18] have previously optimized the microstructure of porous anode, which provide efficient electric contact and gas/water transport between electro catalytic layers and bipolar plates. Percolation theory, which has been used to characterize electro catalytic processes and gas diffusion conditions in fuel cells, was unsuitable for PEMWEs because pores are not randomly distributed in anode. Sung et al. [19] via a platinum-like behavior electro catalyst and solid polymer electrolyte technique used on high concentration of electrochemical ozone water generation, approximately 1.37 ppm at ambient environment by adjusting the voltage range (6–10 V) to set the maximum current at 3 A to satisfy a household demand. Consider the catalyst of membrane will influence the performance of ozone generation. Here, we will observe ozone performance of several materials, such as Pt/IrO₂, Ta/IrO₂, Ru/IrO₂ and Pt/SnO₂.

2. EXPERIMENTAL METHODS

2.1 Ozone Generator and Test System Design

The anode support is an important component of the membrane cell for ozone generation because of that it could provide protection and structure, to promote the electrolysis. In addition to corrosion resistance, it is expected to present excellent electro catalytic activity toward oxygen evolution, good electrical conductivity, electrochemical stability, and low oxygen evolution over potential. The ozone generator was prepared by a proton exchange membrane cell. A Nafion® 117 membrane (MEA), its size of nine cm square, which was used as a solid electrolyte, and the anode support were sandwiched between end plates. A applied voltage exceeding 2 V at the anode combined with high concentrations of oxygen, ozone, and water resulted membrane cell in low pH (pH < 2), promoting electrochemical reactions of electrode materials, such as corrosion, so all components need to use material of ozone-resistant or compatibility with ozone. This test were used porous titanium

coating platinum as the cathode support of cell, and replace the new MEA when individual test over. The end plates were made of titanium plate, to be a cell support structure, and its size of nine cm square. The watertight gaskets were made by silicone, due to its resistance to ozone. Each component was vertical stacked neatly, and then lock with 30 kg per square cm torque. Water was fed to the anode of ozone membrane cell, where oxygen evolution and ozone production occur. The performance of various anode supports during the ozone generation process was examined in a continuous flow system. The test system consisted of a filter, flow meter, ozone generator (membrane cell), byproduct tank, mixing tank, and ozone concentration detector (Fig. 1). Water was purified through the filter and entered the ozone membrane cell at a constant flow rate set using the flow meter. Products such as O_2 and O_3 went through the mixing tank and the produced ozone was detected using an ORP-15 ozone concentration detector. The experimental conditions, such as applied voltage (4 V) and water flow rate (15 L h^{-1}), were maintained constant during this test. The ozone membrane cell was assembled and linked to the data acquisition system, which recorded the electrical characteristics. All anode supports were installed between the membrane anode side and the end plate of cell for testing.

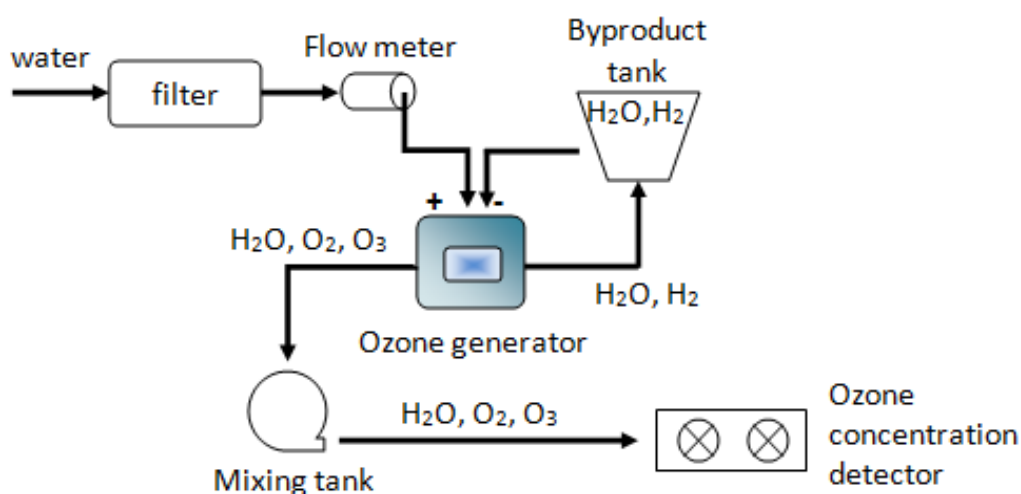


Figure 1. Experimental setup for anode performance test.

2.2 Anode Support Preparation

The materials of anode support usually include stainless, carbon and noble metal, such as Ta, Nb, Zr. Ismael Goncalves et al. [20] use stainless steel fine mesh (AISI304, $AG = 4.0 \text{ cm}^2$, $\varnothing = 0.125 \text{ mm} \times 0.125 \text{ mm}$ and $= 0.075 \text{ mm}$) to be anode support, and composed of tin dioxide containing antimony. Khalid Zakaria et al. [21] prepare anode support by dipcoating Ni/Sb-SnO₂ onto $7.0 \text{ cm} \times 5.0 \text{ cm}$ Ti mesh. Further, Lirong Ma et al. [22] show that based on catalysis efficiency of Amperes per milligram of Ir, the Ir/TiC catalyst is found to be more active than unsupported Ir catalyst. It could be summarized that catalyst supported be more active and the anode support need porous characteristic. Literature data [18-24] show that thermal sintering of spherically shaped titanium powder was typical preparation method. The sintering of spherical particles can make structures having densities close to

those of solid phases (from 0.553 up to 0.641). Reference parameters are listed on Table 1.

Table 1. The reference parameters of Ti thermal sintering.

Parameter item	value
Pore size	5-30 μm
Particle size	25-250 μm
Gas Permeability	$1 \times 10^{-13} - 1 \times 10^{-11} \text{ m}^2$

A selection of three commercial iridium oxide (IrO_2) series anode support, including Pt/ IrO_2 , Ta/ IrO_2 , and Ru/ IrO_2 , will be compared with the Pt/ SnO_2 ozone anode support. The Pt/ SnO_2 ozone anode support was prepared by porous plate of thermally sintered Ti powder. The particle size of titanium powder was under 100 μm and thermo sintering into a plate over 650 $^\circ\text{C}$, to be anode support. The parameters listed in Table 2.

Table 2. The parameters of the Pt/ SnO_2 ozone anode support.

Parameter item	value
Pore size	30 μm
Particle size	100 μm (max)
Gas Permeability	$2 \times 10^{-12} \text{ m}^2$
Surface roughness(Ra)	6.26 μm
Surface roughness(Rz)	52.93 μm

First, the sintered Ti of anode support was coat with catalyst (Pt/C), to increase the reaction of activity. The loading of Pt was 0.18055 mg/cm^2 . The Pt-Ti based anode support will be analysis by energy-dispersive X-ray spectroscopy (EDS) to confirm composition. The EDS compositional analysis of the anode is shown in Fig. 2, and elemental contents are listed in Table 3. And then the anodes were prepared following a procedure based on that of Wang et al [25].

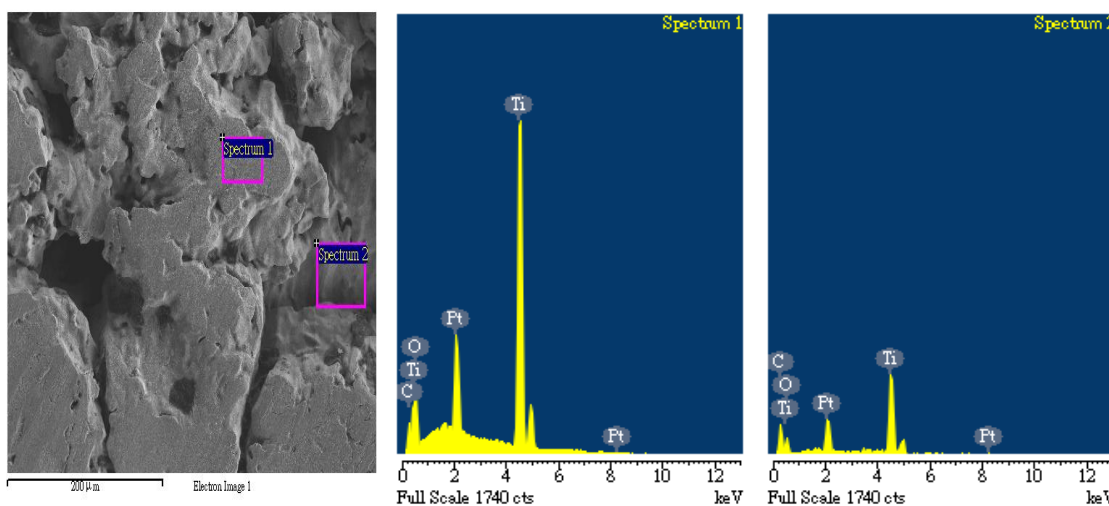


Figure 2. EDS compositional analysis of Pt-Ti based support.

Table 3. Elemental composition of the Pt-Ti based ozone anode support.

Element		C	O	Ti	Pt	Total
Weight(%)	Spectrum 1	2.21	9.46	72.36	15.98	
	Spectrum 2	9.23	10.01	62.66	18.10	
	Std. deviation	4.96	0.39	6.85	1.50	
	Mean	5.72	9.73	67.51	17.04	
					100.00	

3. RESULTS AND DISCUSSION

3.1 SEM & EDS Analyses

All above ozone anode support were analysis by scanning electron microscopy (SEM) to observe their surface morphologies. The surface morphologies of the Pt/IrO₂, Ta/IrO₂, Ru/IrO₂ and Pt/SnO₂ were examined by SEM.

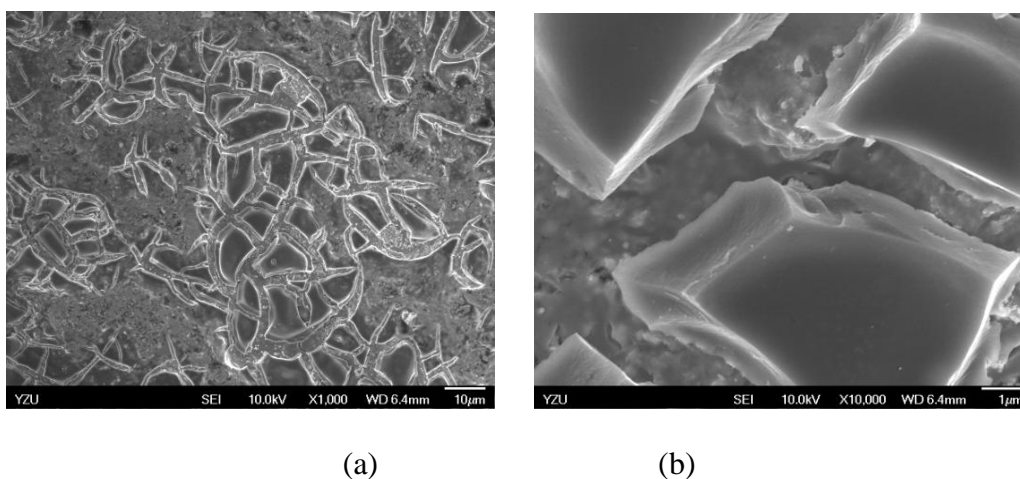


Figure 3. SEM morphologies of the Pt/IrO₂ anode support (a) 1,000× (b) 10,000×.

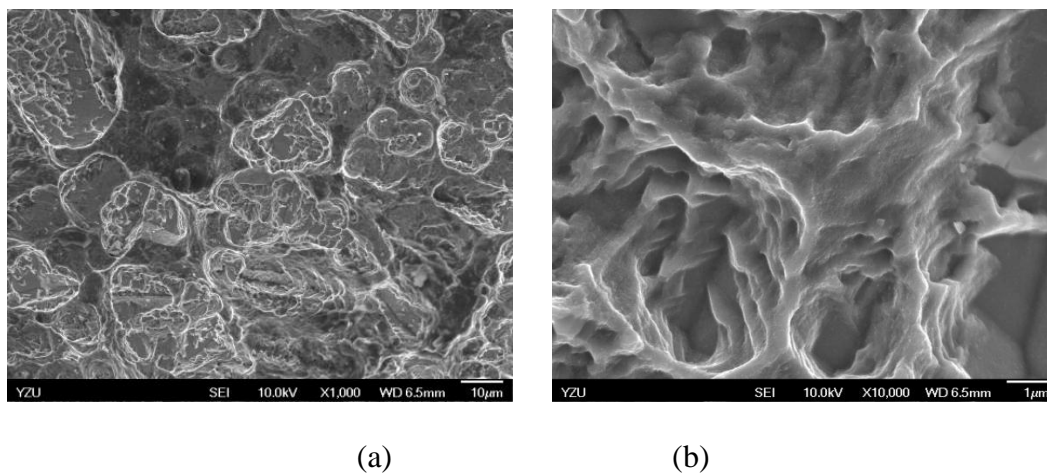


Figure 4. SEM morphologies of the Ta/IrO₂ anode support (a) 1,000× (b) 10,000×.

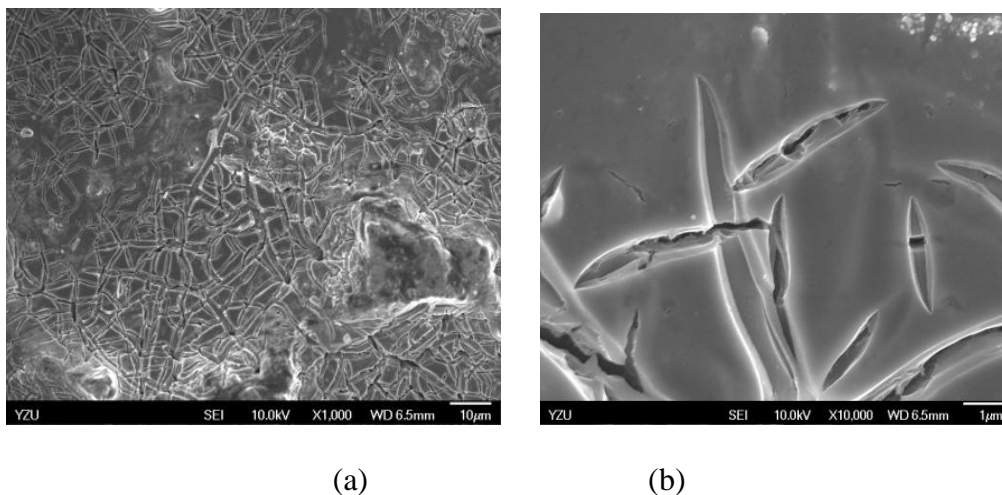


Figure 5. SEM morphologies of the Ru/IrO₂ anode support (a) 1,000× (b) 10,000×.

It could observe the catalyst how to distribute on the substrate and to know the relationship in electrochemical reaction for ozone generation. Fig. 3(a) and 3(b) appears the SEM micrograph of the Pt/IrO₂ anode support surface in different the magnification of 1,000× and 10,000×. It show the Pt/IrO₂ catalyst exhibited mesh-like patterns over the substrate. It was similar the IrO₂/Ru anode surface morphologies was shown in Fig. 5(a). At 10,000× magnification, it could be observed cracks on the substrate surface, albeit with different sizes (Figures 3(b) and 5(b)). The Ta/IrO₂ anode displayed Groups (Figure 4(a)) and significantly jagged pore structures (Figure 4(b)).

The SEM surface morphology of Pt/SnO₂ ozone anode support is shown in Figure 6. Figure 6(a) clearly revealed the porosity of the substrate surface, which presented densely, distributed small white particles within the pores (Figure 6(b)) and catalyst particles densely distributed at 30,000 × magnifications (Figure 6(c)).

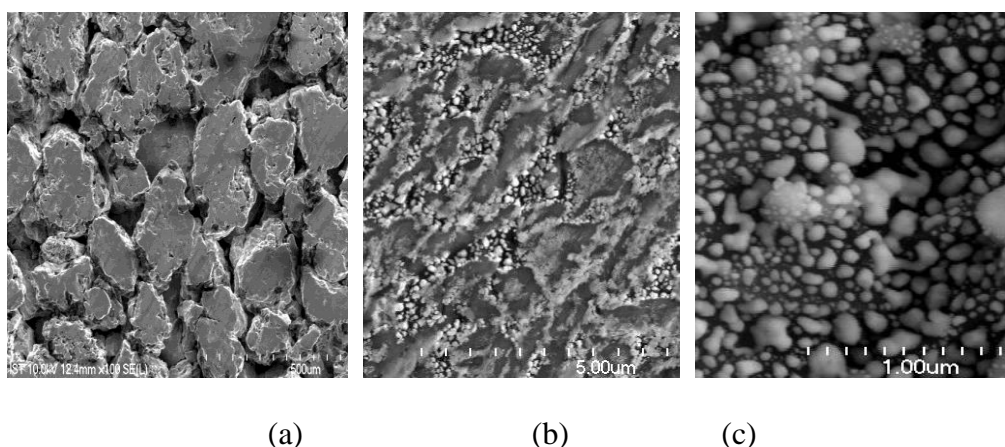


Figure 6. SEM morphologies of the Pt/SnO₂ anode support (a) 1,000× (b) 10,000× (c) 30,000×.

The micro porous structure of the anode facilitated the electrolyte penetration into the catalyst layer of the membrane and the electrolysis. In turn, the generated gas, ozone, was discharged through the pores. At 10,000× magnification, SEM images showed that the catalyst particles adhered to the

anode surface and were distributed. At 30,000× magnification, the catalyst particles of approximately 50–100 nm were clearly attached to the surface. The EDS compositional analysis of the anode is shown in Fig. 7, and elemental contents are listed in Table 4. These results indicated that major component are titanium, platinum and minor component are tin, oxygen and carbon, contents amounted to 51.3%, 24.71%, 8.75%, 6.34%, and 7.62%, respectively. The Pt/SnO₂ ozone anode support will sequentially be investigated with Pt/IrO₂, Ta/IrO₂, and Ru/IrO₂ in terms of ozone electrochemical characteristics.

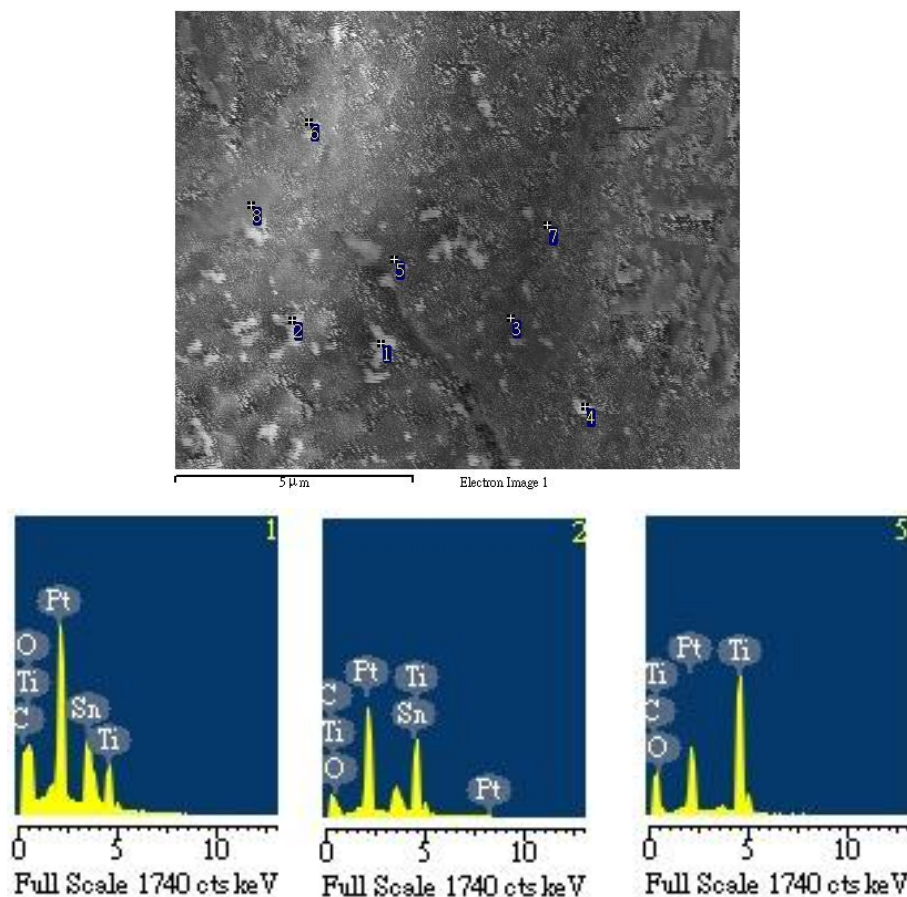


Figure 7. EDS compositional analysis of Pt/SnO₂ anode support.

Table 4. Elemental composition of the Pt/SnO₂ ozone anode support.

Element	C	O	Mg	Si	Ti	Sn	Pt	Total
Weight(%)	7.62	6.34	0.37	0.92	51.30	8.75	24.71	100.00

3.2 Ozone concentration

The produced ozone concentration (in mg dm⁻³), a key indicator performance of the anode support in membrane cell, was determined by individual mention ozone anode support. The results are shown in Fig. 8. All these anode supports react within half hour to generate ozone. The performance of Ta/IrO₂ anode support was best between iridium oxides (IrO₂) series, but the ozone concentration still is lower than Pt/SnO₂ anode support. It was possible that doped catalyst of SnO₂ at the anode has greater effect about enhance the activation of the ozone generation reaction and stifle the kinetics of oxygen evolution reaction. This ozone concentration in the solution phases was lower than that observed by Wang et al. [25], who reported 19 mg dm⁻³, and Zakaria et al. [21], who reported 20 mg dm⁻³. These differences were mainly due to the anolyte pumped through the cell, air breathing cathode and different NATO anode area (4cm × 6cm Ti mesh 50% open area, and 7cm × 5cm Ti mesh 50% open area). It could still prove Ni/Sb-SnO₂ anode show high performance for the generation ozone at room temperature.

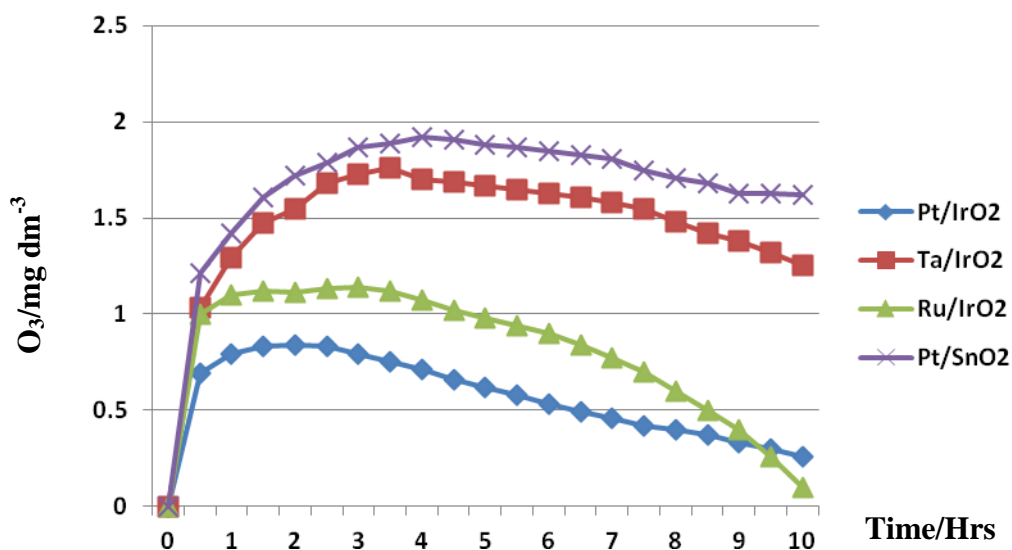


Figure 8. Produced ozone concentration for various anode supports.

3.3 Ozone Current efficiency and Density

Water generates oxygen through an electrochemical oxidation reaction. When applied voltage 4 V at the anode was thermodynamically more favorable about the ozone reaction, According to formation reactions (1)-(3) and Faraday’s law, the ozone current efficiency can be calculated follow as [26]:

$$\eta = \left(\frac{nFM}{C} \right) \times 100\% \tag{4}$$

Where n is equal to 6, the moles of electrons transferred for one mole of ozone production and according formation reactions (2), F is Faraday’s constant and equal to 96,485 C/mol, M is the mole of ozone generated by the cell, and C is the amount of electric charge input into the cell, and it can be calculated from the current values recorded from the power supply. Figures 9(a) and 9(b) show data from the experiment using different anode support as Pt/IrO₂, Ta/IrO₂, Ru/IrO₂ and Pt/SnO₂ ; 9(a) shows plots of current efficiency against time and 9(b) the corresponding plot of current density. The anode support of Pt/SnO₂ present a best current efficiency result was ca. 26%, and it was less than Parsa and Abbasi reported a maximum ozone current efficiency of 53.7% using 6.3 cm² Ni/Sb-SnO₂ Ti mesh anodes in acid solution, and tending toward steady state values < 20% [27]. The current density of Pt/SnO₂ anode support was tend toward steady state values 0.22A cm⁻², and Pt/IrO₂, Ta/IrO₂ and Ru/IrO₂ was less than Pt/SnO₂. The current density of Pt/SnO₂ anode support kept steady but current efficiency down step by step, it was possible that solution of ozone detect mainly and gas phase ozone missed consider.

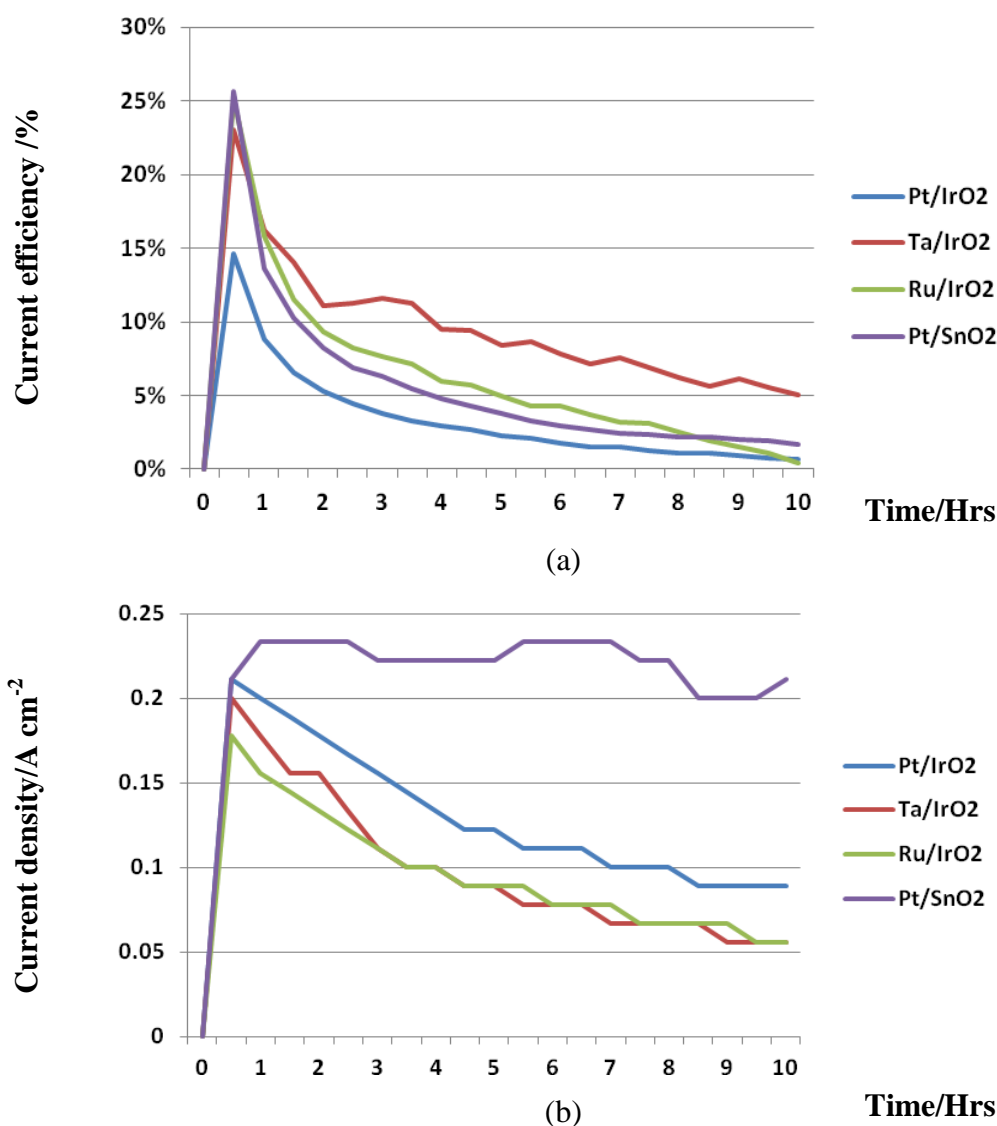


Figure 9. Plot of (a) ozone current efficiency and (b) ozone current density for various anode supports.

3.4 Power consumption

The power consumption per unit of ozone (E_p) was obtained follow as [26]:

$$E_p = (VI) / Q \tag{5}$$

Where Q is the ozone generation rate, I is the applied current value, and V is the cell voltage. As show in Fig. 10, the power consumption varied with time and dramatically increased with decreasing of current efficiency. It is possible that catalyst of anode surface has been poison and lead to the current efficiency decreased with time. In the electrolysis step of water, the oxygen production either directly parallel to ozone production or the subsequent decomposition of ozone to oxygen, and it was mainly result that the loss of current efficiency. Zakaria et al.[21] show the result of power consumption increased with increased voltage and the lowest power consumption equal to 25kwh kg^{-1} when applied voltage 2.5V and highest power consumption equal to 37kwh kg^{-1} when applied voltage 3V. Cui et al.[26] present the lowest power consumption of 48kwh kg^{-1} ozone was achieved at 2V and the highest power consumption of 160kwh kg^{-1} ozone was achieved at 1.6V. It can show that power consumption and voltage no absolute relationship. In this case, the power consumption of Pt/SnO₂ anode was equal to 38 kwh kg^{-1} when the constant voltage 4V was applied. Compare Pt/SnO₂ with Ta/IrO₂ anode, Ta/IrO₂ anode has lower power consumption and higher current efficiency, and it seem to show the Pt/SnO₂ anode relatively poor performance in high overvoltage.

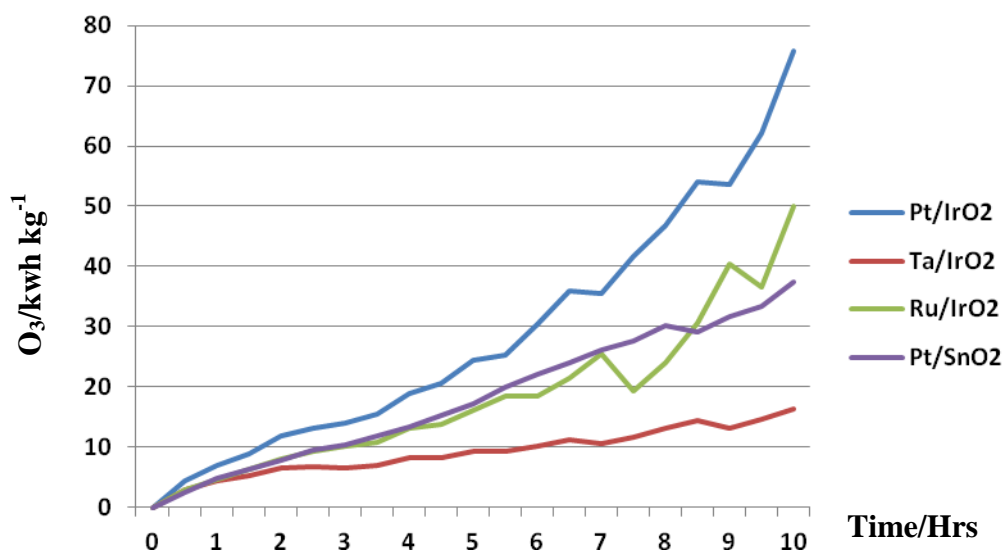


Figure 10. Plot of power consumption for various anode supports.

3.5 Long Term Test

Figure 11 shows the results of a durability study to evaluate the commercial value of anode support. The Pt/IrO₂ anode presented ozone concentration of 0.8 ppm in the beginning and more rapidly decay to zero after 13 hours. The Ta/IrO₂ anode presented ozone concentration of 1.8 ppm in

the beginning and also rapidly decay to zero after 13 hours. The Ru/IrO₂ anode presented ozone concentration of 1.1 ppm in the beginning and also rapidly decay to zero after 13 hours. Compared the Pt/SnO₂ based ozone anode support presented a steady ozone concentration exceeding 1.07 ppm for 200 h. During the electrolysis, ozone generation was characterized by current detection. The current feedback of Pt/IrO₂, Ta/IrO₂, and Ru/IrO₂ anode were the same that current feedback began while ozone generation, but they did not show any reaction after 25 hours. The Pt/SnO₂ based ozone anode support maintained a current feedback of approximately 1.5–2 A for 200 hours before decreasing gradually and the current fluctuations stabilized, but current efficiency approaching to zero. Reference Paul Andrew Christensen et al.[28] use Sb-Doped SnO₂ anode to make a durability study, and the anode failed after ca. 200 hours electrolysis in 1 M HClO₄ at 100mA⁻². These result was similar each other.

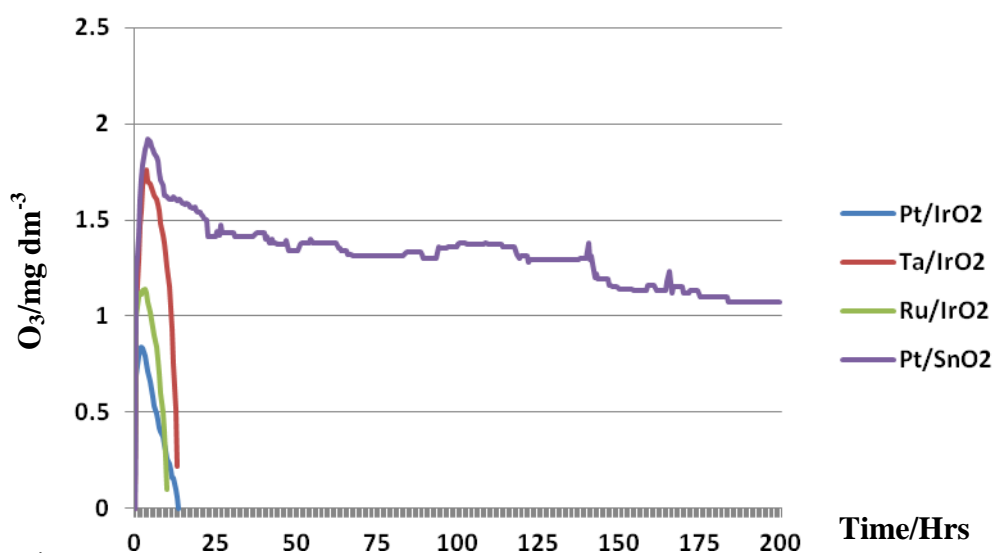


Figure 11. Plots of durability experiment for various anode supports.

4. CONCLUSIONS

PEM water electrolysis is ideal for producing ozone without NO_x formation. The reaction only generates oxygen, ozone, and protons at the anode and hydrogen at the cathode. The quality of the anode support affects the ozone production efficiency. In a high voltage environment, the anode support exhibited an effective electrochemical reaction. Other parameters, such as the surface roughness, noble metal loading, particle size, thermal sintering temperature, and permeability, also need careful consideration. A Pt/SnO₂ based ozone anode support was installed in the membrane anode side of ozone membrane cell, it presented better performance than Pt/IrO₂, Ta/IrO₂ and Ru/IrO₂ anode supports in terms of ozone concentration and electrical characteristics, and show the result that a steady ozone concentration exceeding 1.07 ppm for over 200 h when voltage 4V. It could be confirmed that added anode support in the membrane cell, will enhance cell performance of ozone

generation. The Pt/SnO₂ based ozone anode support reference a procedure based on that of Wang et al [25], could obtain stable ozone concentration and electrochemical performance.

ACKNOWLEDGEMENT

The authors are grateful to the National Science Council, Taiwan, under contract NSC102-2622-E-155-001-CC2 and NSC102-2221-E-155-005-MY3 for the financial support.

References

1. L. S. Wei, J. H. Zhou, Z. H. Wang and K. F. Cen, *Ozone: Science And Engineering*, 29(2007)207–214.
2. P. C. Foller and M. L. Goodwin, *Ozone: Science And Engineering*, (1984) 29–36.
3. S. Stucki, G. Theis, R. Kötzt, H. Devantay and H. Christen, *Journal of The Electrochemical Society*, 132 (1985) 367–371.
4. S. Stucki, H. Baumann, H.J. Christen and R. Kötzt, *Journal of Applied Electrochemistry*, 17 (1987) 773–778.
5. A.A. Babak, R. Amadelli, A. De Battisti and V.N. Fateev, *Electrochimica Acta*, 39 (1994) 1597–1602.
6. A.A. Chernik, V.B. Drozdovich and I.M. Zharskii, *Russian Journal of Electrochemistry*, 33 (1997) 259–263.
7. Y. Beaufils, P. Bowen, C. Comminellis and C. Wenzed, Proceedings of Electrochemical, Society, Abstract No. 617 (1998) 730.
8. Y. Beaufils, C. Comminellis and P. Bowen, Electrochemical Engineering. In *Icheme Symposium Series No. 145* (1999) 191.
9. R.G. Rice and A. Netzer (Eds.), *Handbook Of Ozone Technology And Applications*. 1st ed. Ann Arbor, Mich.: Ann Arbor Science (1982).
10. R. Amadelli, A. De Battisti, D.V. Girenko, S.V. Kovalyov and A.B. Velichenko, *Electrochimica Acta*, 46 (2000) 341–347.
11. Leonardo M. Da Silva, Luiz A. De Fariab and Julien F.C. Boodts, *Electrochimica Acta*, 48 (2003) 699–709.
12. K. Naya and F. Okada, *Electrochimica Acta*, 78 (2012) 495–501.
13. S. Stucki, G. Theis, R. Kotz, H. Devantay and H.J. Christen, *Journal Of The Electrochemical Society*, 132 (1985) 367–371.
14. K. Kitsuka, K. Kaneda, M. Ikematsu, M. Iseki, M. Mushiake and T. Ohsaka, *Journal Of The Electrochemical Society*, 157 (2010) 30–34.
15. S. Cheng and K. Chan, *Electrochemical And Solid-State Letters*, 7 (2004) 4–6.
16. Marina Shestakova, Pedro Boneteb, Roberto Gómezb, Mika Sillanpääa and Walter Z. Tang, *Electrochimica Acta*, 120 (2014) 302–307.
17. Marcelo carmo, David L.Fritz, Jurgen Mergel and Detlef Stolten, *International Journal of Hydrogen Energy*, 38 (2013) 4901–4934.
18. S.A. Grigoriev, P. Millet, S.A. Volobuev and V.N. Fateev, *International Journal of Hydrogen Energy*, 34 (2009) 4968–4973.
19. C. C. Sung, C. Y. Liu, H. C. Huang, L. H. Hu, *Journal Of Solid State Electrochemistry*, 12 (2012) 3923–3928.
20. Ismael C. Gonc, alves, Wallans T.P. dos Santos, Débora V. Franco, Leonardo M. Da Silva, *Electrochimica Acta*, 121(2014) 1-14.
21. Khalid Zakaria, Paul Andrew Christensen, *Electrochimica Acta*, 135(2014) 11-18.
22. Lirong Ma, Sheng Sui, Yuchun Zhai, *International journal of hydrogen energy* 34 (2009) 678–684.

23. A.B. LaConti, A. Fragala, J. Boyack J, JDE. McIntyre, S. Srinivasan, F.G. Will, *The Electrochemical Society Proceeding Series 77* (1977) 354.
24. H.Y. Jung, S.Y. Huang, P. Ganesan, B.N. Popov, *Journal Of Power Sources* 194 (2009) 972-975.
25. Y.-H. Wang, S. Cheng, K.-Y. Chan, and X.Y. Li, , *J. Electrochem. Soc.*, 52(11) (2005)D197–D200.
26. Yuhong Cui, Yubhai Wang, Bin Wang, Haihui Zhou, Kwong-Yu Chan, and Xiao-Yan Li, *J. Electrochem. Soc.*, 156(4) (2009)E75–E80.
27. J. B Parsa and M. Abbsai, *J solid State Electrochem*, 16,1011(2012)
28. Paul Andrew Christensen, Khalid Zakaria, Henriette Christensen, and Taner Yonar, *J. Electrochem. Soc.*, 160(8) (2013) H405–H413.

© 2016 The Authors. Published by ESG (www.electrochemsci.org). This article is an open access article distributed under the terms and conditions of the Creative Commons Attribution license (<http://creativecommons.org/licenses/by/4.0/>).